Food Sterilization by Electrical Heating: Sensitivity to Process Parameters

L. Zhang and P. J. Fryer
Dept. of Chemical Engineering, University of Cambridge, Cambridge, CB2 3RA, England

The design of efficient continuous sterilization equipment for flowing solid-liquid food mixtures requires that temperature and velocity distributions within the fluid are known. In electrical (ohmic) heating, electric current is passed through a two-phase mixture, and heat generated as a result of the resistance of the food acts to sterilize it. This allows rapid sterilization of solid-liquid mixtures which minimizes quality loss. A computational process model simulates the effect of realistic physical property changes. The effect of variations in physical properties can have a significant effect on the temperature of the product and thus on its sterility. Realistic designs will have to cope with temperature differences between phases. Experimental data for velocities in a food flow have been incorporated into an enthalpy balance model for heat transfer in solid-liquid mixtures. The effect of inlet temperature on the length of hold tube required to give the necessary process sterility calculated shows the variation in output conditions that might result in real systems.

Food Sterilization

The aim of food sterilization is to produce a sterile product of the highest possible quality. The classical method is canning, in which the product is sealed and then processed until it has reached the correct level of sterility. This may result in a low-quality product; the kinetics of sterilization and quality loss reactions are such that a better product is obtained by heating to higher temperatures for shorter times. This is best done in a continuous process with three sections: (i) a *heating* section in which product is first heated to the required temperature; (ii) a *holding* section in which it is held at temperature long enough to ensure sterility; and (iii) a *cooling* section prior to packaging. The holding section is generally a horizontal or slightly inclined tube.

Continuous processes are capable of producing a higher-quality product than canning. It is possible to process liquids, using forced convective heat transfer, at much higher heating and cooling rates, on the order of 1°C/s, than is possible in processes which rely on thermal conduction or natural convection in the can. A number of commercial food sterilization processes involve the transport and heating of solid-liquid food mixtures of high solids fractions (Holdsworth, 1993). These flows can consist of up to 50-60% solids, particle diameters up to 25 mm in diameter, and carrier fluids which are generally non-Newtonian. Fluid velocities are restricted by the requirement to cause as little damage as possible to the mixture. It is difficult to process solid-liquid mixtures rapidly as solids heating is thermal-conduction-controlled; however, new volumetric heating technologies, such as microwave (Ayappa et al., 1991) and electrical (ohmic) heating (Biss et al., 1989; Parrott, 1992) allow solids to be heated at the same rates as liquids.

Volumetric processes potentially remove heat-transfer limitations on processing particles during the heating stage. Despite this, Zhang and Fryer (1993) demonstrate that significant quality loss can still accumulate during cooling. It is thus vital to study the whole process. To design processes and confirm the sterility of the final product, the temperatures of solid-liquid mixtures must be known. Little information is available on the heating rates of the particles and the liquid and of the flow patterns of the food mixture; the design of plant is thus largely empirical. Food will have a range of residence times in any flow situation, and so the process must be designed so that the fastest moving piece of fluid must be sterilized while the slowest moving part is not overcooked.

The APV Baker ohmic heater forms the basis for the electrical heating system modeled here. As described by Parrott (1992), the heater consists of a vertical or near-vertical tube up to 10 m in length and 75 mm in diameter, containing a series of up to seven electrode housings, each containing a single cantilever electrode across the tube. Up to 3 ton/h of flood flow upward through the tube past the electrodes; current density is much higher in the connecting tubes than in the electrode housings, so the majority of the heating occurs in

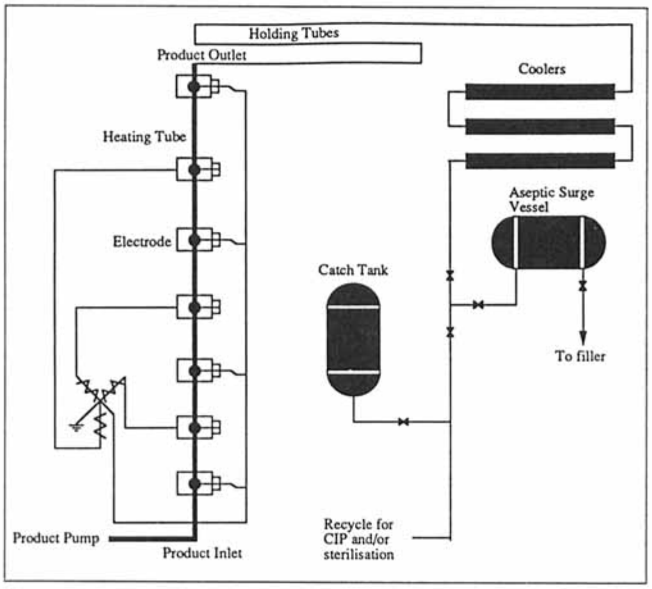

Figure 1a. Flowsheet APV Baker 'ohmic heater' process from Parrott (1992).

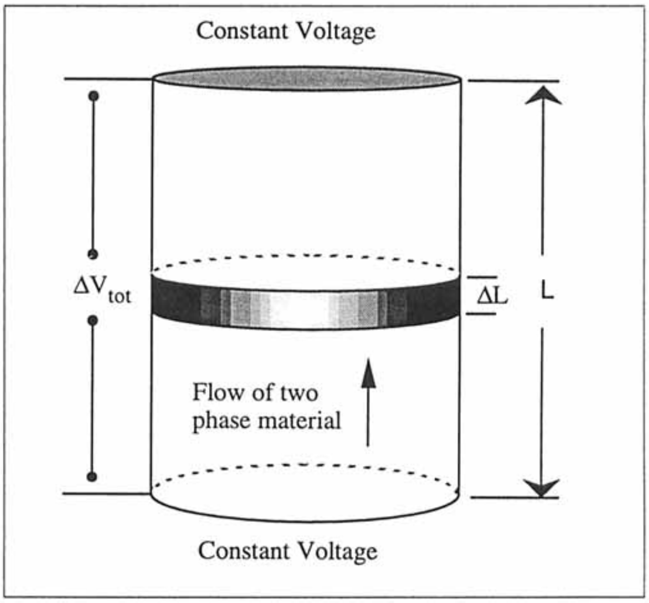

Figure 1b. Tubular system, connecting two electrodes modeled here.

the tube. The food is heated to temperatures in the region of 130–140°C, where sterilization is rapid; the system is pressurized so that boiling does not occur. Figure 1a shows a schematic diagram of the process flowsheet.

In the commercial process, a two-phase mixture is first heated in vertical flow and then held and cooled in horizontal flow. Most published work on the conveying of solid-liquid mixtures considers high-density solids in turbulent water flows, such as the conveying of coal in water (for example, see Wilson, 1991). In contrast, food flows involve non-Newtonian fluids and are of low Reynolds number; although there is extensive literature on the flow of very low-Reynolds-number suspensions, it is difficult to apply this knowledge to the high solids fractions and particle-particle interactions found in food flows. The flow of single-phase food liquids through process plant has been thoroughly studied, for example, by Rao and Loncin (1974), Heppell (1985), and Sancho and Rao (1992), and theoretical solutions for the flow of single-phase fluids are available, such as those of Sawinsky and Simandi (1982). Studies of suspensions are described by Singh and Lee (1992). It is possible for particles to travel faster than the mean fluid velocity if they are suspended; theoretically, in fully developed Newtonian laminar flow, particles at the center line might travel twice as fast as the mean flow. This assumption is commonly used in the process plant to ensure sterility. Dutta and Sastry (1990a,b) studied velocity distributions in flows of up to 0.8% by solids volume. Singh and Lee (1992) study flows of more realistic concentrations, of up to 40% solids, in a scraped surface heat exchanger, and identified effects due to both system orientation and fluid viscosity.

In the electrical heating process, a wide range of food temperatures are possible, depending on the particle electrical conductivity and residence time within the heater; de Alwis and Fryer (1992) have demonstrated the effect of electrical conductivity and particle orientation on the electrical heating rate. To be of maximum relevance to commercial practice, experimental information is needed to allow models to be verified. Zhang and Fryer (1993) describe a model for the electrical heating of a mixture, assuming constant physical properties, which first finds the heat generation within a unit cell of material and shows how particle and fluid velocities might be incorporated to predict the temperature distribution. Here, the model is extended to take account of the temperature dependence of the physical properties of food materials, especially the electrical conductivity. A robust finite difference scheme has been developed to simulate the complex heating patterns that can result from nonlinear physical properties, and correlations of heat generation data given. The model uses two sets of data: (i) for particle flow, obtained experimentally in a collaboration between workers at Cambridge and Compiegne; (ii) for the physical properties of food materials, obtained at Cambridge and elsewhere, to demonstrate the effects which may arise in real systems.

Electrical Heating Model

To solve the problem of electrical heating requires simultaneous solution of the coupled equations for the electric, thermal, and flow fields. This requires an unacceptable amount of computer capacity. Here, a series of approximations have been made to simplify the problems to the point where it can be solved computationally.

(i) Heat transfer and generation equations for the solid and liquid phases have been modeled by a one-dimensional heat balance; differences between the velocities of the phases can be accommodated.

(ii) Heating in the electrode housing is neglected. The heating of food during flow through the vertical tube connecting two electrodes is modeled. Boundary conditions of uniform voltage across the entrance and exit of the tube (Figure 1b) are defined for solution of the electrical field. As the mixture flows up the tube, the temperature—and thus the electrical conductivity—of the two phases changes. The voltage gradient will thus vary up the tube, and an iterative calculation is necessary.

(iii) The tube is modeled as a series of sections. Within each section, the solid-liquid mixture has been represented as a uniform lattice of spherical particles on a regular grid, such that a unit cell of the material can be modeled as representative of the whole, an approach common in symmetrical systems (McKie and McKie, 1986). It is assumed that in each section of the tube, heat generation rates in the solid and liquid, the temperatures of the phases, and velocities of the phases are uniform and known. Fryer et al. (1993) show that uniform heating in the liquid is possible, and Zhang and Fryer (1993) show that a rotating particle can heat uniformly.

Thermal balances on solid and liquid phases

Using the above assumptions, the response of the system can be modeled to a set of thermal balances. An enthalpy balance for a particle can be written:

$$-ha(T_S-T_L)+Q_S=v_S(\rho c_p)_S\frac{dT_S}{dx} \qquad (1)$$

where h is the convective heat-transfer coefficient between particle and liquid, a is the area of the particle per unit volume ($6/d_p$ for a sphere of diameter d_p), and Q_S is the heat generation rate per unit volume of solid. This can be rewritten as:

$$-H_S(T_S-T_L)+G_S=v_S\frac{dT_S}{dx} \qquad (2)$$

where $H_S=ha/(\rho c_p)_S$ is a modified heat-transfer term and $G_s=Q_S/(\rho c_p)_S$ is the inherent heating rate for electrical heating in the absence of heat transfer.

Assuming no heat loss at the tube wall, the liquid-phase heat balance becomes:

$$\frac{\phi}{(1-\phi)}ha(T_S-T_L)+Q_L=v_L(\rho c_p)_L\frac{dT_L}{dx} \qquad (3)$$

where ϕ is the fraction of the volume of the system occupied by the solid, and Q_L is the heat generation rate per unit volume of liquid. This can be written:

$$H_L(T_S-T_L)+G_L=v_L\frac{dT_L}{dx} \qquad (4)$$

where $H_L=[\phi/(1-\phi)][ha/(\rho c_p)_L]$ and $G_L=Q_L/(\rho c_p)_L$.

To find the temperatures of the two phases, Eqs. 2 and 4 must be solved together; data for heat generation rates, particle and fluid velocities, and heat-transfer coefficients must be known.

Solution of Laplace's equation for heat generation rates

To find the voltage distribution in the heater, it is necessary to solve Laplace's equation:

$$\nabla\cdot(\kappa\nabla V)=0 \qquad (5)$$

where V is voltage throughout the medium. The electric field intensity, $E=-\text{grad}\ V$, and the heat generation at each point $Q=\kappa\ E\cdot E$ can then be calculated.

Except in very limited conditions where κ is constant (de Alwis et al., 1989) Eq. 3 cannot be solved analytically. Here, it is necessary to model the field in sections of the connecting tube (Figure 1b) with boundary conditions of constant voltage at the top and the bottom of the tube.

Various approaches have been taken to estimate the field distribution within solid-liquid food mixtures. Sastry (1992) approximates the mixture as a set of series and parallel resistances. This approach, however, incorrectly assumes that all current lines are parallel to streamlines. The current paths around objects may be complex, as demonstrated by de Alwis et al. (1989) (for spheres) and de Alwis and Fryer (1992) (for more complex shapes); Zhang and Fryer (1994) demonstrate that circuit analysis models can be inaccurate in some situations.

Zhang and Fryer (1993) describe a model which assumes that the food mixture is homogeneous, such that sections of the fluid can be modeled as representative of the whole. If the distribution of particles in the liquid is uniform, the system can be divided into a number of 'unit cells,' each containing a number of particles. It is only necessary to model one cell to predict the behavior of the whole. Figure 2 shows a possible cell pattern in which particles are distributed on a cubic lattice.

The cells in Figure 2 form a regular symmetric pattern; due to internal symmetry, only one-eighth of the cell needs to be simulated, as shown also in the figure. The system is symmetrical, so the boundary conditions in the cell are similar to those of the whole system: (i) there is no current flow through the side surfaces, so the wall of the pipe can be assumed to be there; (ii) constant voltage over the top and bottom surfaces. The model is thus appropriate to the adiabatic flow of particles in tubular geometries. The cell size can be adjusted for any solids fraction, as discussed by Zhang and Fryer (1993). A commercial program, ANSYS (Swanson Corp., Houston, PA), has been used to solve Laplace's equation in the unit cell as a function of solids fraction and the ratio of solid to liquid electrical conductivity, $R_\kappa=\kappa_S/\kappa_L$.

To solve Eqs. 2 and 4 it is necessary to obtain the mean heat generation rates in each phase. It was found convenient to define ratios of the local heat generation rate at a point relative to the heat generation that would result if only the liquid were present, Q_1:

$$Q_1=\kappa_L E^2 \qquad (6)$$

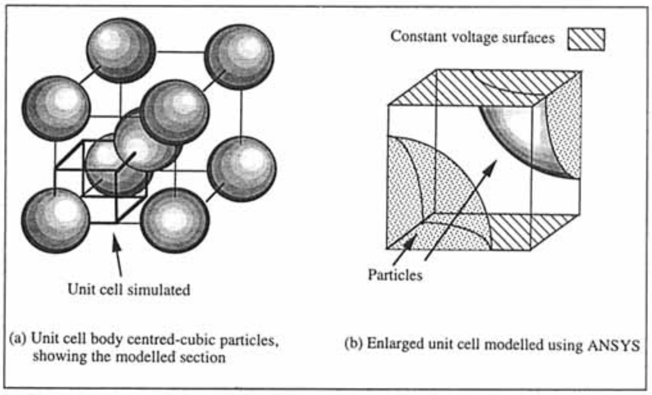

(a) Unit cell body centred-cubic particles, showing the modelled section

(b) Enlarged unit cell modelled using ANSYS

Figure 2. Unit cell model for particle-liquid mixtures.

where the mean voltage gradient E is here defined as the scalar $\Delta V/\Delta x$, where ΔV is the voltage drop between the two faces of the unit cell, a distance Δx apart.

$$R_Q=\frac{Q}{Q_1} \tag{7}$$

Zhang and Fryer (1993) gave plots of the heat generation ratios R_Q in the two phases using the unit cell model and gave a sample calculation for the solution of the heating of a system of constant physical properties. Here, correlations for the data are developed which can be used in the two-phase thermal balance model.

Before that is done, however, the sensitivity of the calculation resulting from the strong temperature dependence of the sterility and quality of the food shall be demonstrated by an idealized example. For a single-phase system of constant physical properties, neglecting heat transfer:

$$\frac{dT}{dt}=G=\frac{Q}{\rho c_p} \tag{8}$$

giving the design exit temperature:

$$T_e=T_o+Gt_{\text{proc}} \tag{9}$$

after some process time t_{proc}. Depending on G, the time to reach the output temperature can vary. The effect of a process on food sterility is generally quantified by the integrated lethality, or F value (Holdsworth, 1993) defined as:

$$F=\int_0^t 10^{T(t)-T_{\text{ref}}/z}dt \tag{10}$$

where standard food industry values are $T_{\text{ref}}=121.6°\text{C}$ and $z=10°\text{C}$ (Holdsworth, 1993). An F value of 3 min corresponds to a reduction in bacterial spore content by a factor of 10^{12}. The sensitivity of sterility to the temperature can be demonstrated by studying the effect of a fractional change ϵ in G, a temperature profile given by $T=T_o+G(1+\epsilon)t$, for which Eq. 10 can be integrated to give:

$$\Delta F=\frac{e^{\delta_F(T_o-T_{\text{ref}})}}{\delta_F G}\left[\frac{\exp\delta_F(1+\epsilon)(T_e-T_o)-1}{1+\epsilon}+1-\exp\delta_F(T_e-T_o)\right] \tag{11}$$

where ΔF is the change in the calculated F value and $\delta_F=\ln 10/z$. Calculations were carried out to simulate the heating of a material from 20°C to 140°C for various G and thus $t_{\text{proc}}=(T_e-T_o)/G$. Significant changes in the sterility value at the output can be found for small ϵ. The lower the G, and thus the larger the process time, the greater the change in F resulting from a given ϵ. As an example, if $\epsilon=0.05$ and $G=0.5°\text{C/s}$, then an extra 40 min of F can be accumulated through the column; this corresponds to very severe overprocessing.

Using the two-phase model, if data for Q is available, then it is simple to predict temperatures. However, Eq. 11 and the above argument show that it is vital to use a modeling technique which minimizes temperature errors to avoid large errors in the final sterility value. Food physical properties, especially electrical conductivity, are complex functions of temperature; as the ratio of the electrical conductivities changes, the heating rates in the two phases will change. To predict the heating rates of a realistic mixture using the two-phase model it is necessary to predict heating rates accurately as a function of the solid fraction ϕ and the conductivity ratio R_κ. This could best be done by incorporating solution of Laplace's equation for the unit cell into the calculation, but this is highly expensive computationally; here, correlations have been sought which accurately represent unit cell data found by ANSYS. These equations avoid the need to solve the electrical field equations in a complex geometry as part of some iterative scheme, and thus reduce the computational complexity of the problem.

An extensive series of calculations have been carried out for spheres in different situations (Zhang and Fryer, 1993), for $0.5<R_\kappa<5$, and $0.1<\phi<0.68$ (0.68 is the limiting solids fraction for close packing of spheres). Data for volume average heating rates have been correlated. Care must be taken in selecting the form of a correlation. A correlation based on a realistic assumption tends to ensure a better fit to data; for example, the simple physical analysis of gases, which leads to the Van der Waals equation, is still the basis of better correlations for equations of state of realistic gases than is the virial power series equation. Such an analysis has been sought here. de Alwis et al. (1989) note that for a single sphere in an infinite medium, potential theory gives:

$$R_{QS}=\frac{9R_\kappa}{(R_\kappa+2)^2} \tag{12}$$

This effectively corresponds to the limit of $\phi=0$. When the solids fraction is unity, however, from the definition of Eq. 7:

$$R_{QS}=R_\kappa \tag{13}$$

For a finite solids fraction the heating rate will lie between these two values. Data have been correlated in terms of:

$$R_{QS}=\frac{9R_\kappa}{(R_\kappa+2)^2}[1-f_1(\phi,R_\kappa)]+f_1(\phi,R_\kappa)R_\kappa \tag{14}$$

where the function $f_1(\phi, R_\kappa)$ is fitted between the required limits. To find $f_1(\phi, R_\kappa)$, Eq. 14 was first rewritten as:

$$f_1(\phi,R_\kappa)=\frac{R_{QS}-\dfrac{9R_\kappa}{(R_\kappa+2)^2}}{R_\kappa-\dfrac{9R_\kappa}{(R_\kappa+2)^2}} \tag{15}$$

and a polynomial of the form

$$f_1(\phi,R_\kappa)=a_1+a_2\phi+a_3R_\kappa+a_4\phi R_\kappa+a_5\phi^2R_\kappa \tag{16}$$

was fitted to ANSYS data for R_{QS} for $0.5<R_\kappa<2$, and $0.1<\phi<0.68$. Parameters found by least-square fitting were: $a_1=0.110$, $a_2=0.897$, $a_3=-0.03$, $a_4=-0.280$, and $a_5=0.280$.

relative error between the R_{QS} given by the correlation and that calculated by ANSYS solution of Laplace's equation was less than 1%.

The same approach was used to model the liquid. In the limit of $\phi=1$, Eq. 13 applies, while for $\phi=0$, $R_{QL}=1$. The same form of correlation was used:

$$R_{QL}=f_2(\phi, R_\kappa)(R_\kappa-1)+1 \tag{17}$$

$f_2(\phi, R_\kappa)$ was then fitted to the same form of equation as Eq. 16. A relative error below 2% was found for the following: $a_1=0.005$, $a_2=0.43$, $a_3=0.009$, $a_4=-0.04$, $a_5=0.250$ for the range $0.5<R_\kappa<2$ and $0.1<\phi<0.68$.

Solution technique for temperature-dependent physical properties

In a real food fluid, the electrical conductivities of the two phases will both be functions of temperature; in practice, it is commonly assumed that κ is a linear function of temperature, as in Eq. 18:

$$\kappa=k_o+k_1T \tag{18}$$

The commercial process heats material from a known temperature to a required outlet temperature for sterilization; the temperature boundary conditions, of the inlet temperatures of the solid, T_S^o, and liquid T_L^o, and the required outlet temperature, T_{OUT}, will thus be known. As noted below, the outlet temperature is used to obtain a first estimate for system electrical conductivity.

Equations 2 and 4 for nonuniform physical properties can be solved using Eqs. 6, 16, and 17 to produce data for heat generation. However, to use the heat generation correlations and thus calculate the temperatures, it is necessary to know the field strength in each section of the tube. Due to the variation up the tube, the field strength in any section cannot be determined from the overall voltage difference; an iterative solution is thus necessary.

Although the voltage gradient will vary up the tube, the total current in the commercial system will be constant at steady state, as will the mean current density, defined as the total current divided by the tube cross-sectional area. The mean current density can thus be used as a convergence parameter for the model.

The other useful parameter is the effective electrical conductivity of the mixture, κ_{eff}, defined in terms of the volume average heat generation rate:

$$Q_S\phi+Q_L(1-\phi)=\kappa_{\mathrm{eff}}E^2 \tag{19}$$

which can be written as a ratio, $R_{\kappa\mathrm{eff}}=\kappa_{\mathrm{eff}}/\kappa_L$, by dividing by Eq. 6:

$$R_{\kappa\mathrm{eff}}=R_{QS}\phi+R_{QL}(1-\phi) \tag{20}$$

so that Eqs. 16 and 17 can be used in Eq. 20 to give the effective conductivity ratio.

The iterative procedure is as follows:

(i) A first guess of the current density is obtained assuming that the column is filled only with liquid at the arithmetic mean of the inlet and outlet temperatures, so κ_L is known. This gives a constant voltage gradient up the tube, $E=\Delta V_{\mathrm{tot}}/L$. The heating section is divided into N sections, each of length $\Delta L=L/N$; the voltage drop across each section is thus equal to $\Delta V/N$.

(ii) Consider some section j, where the inlet solid and liquid temperatures, T_S^{j-1} and T_L^{j-1} are known. The voltage drop, ΔV_j, across the section is known, so that the mean field strength is equal to $E_j=\Delta V_j/\Delta L$, using the definition of Eq. 6. It is then possible to find R_κ and the heat generation rates in the two phases using Eqs. 16 and 17. If the physical properties of the materials are assumed constant in the section, then the analytical solution of Eqs. 3 and 5 (Zhang and Fryer, 1993) can be used to find the outlet temperatures T_S^j and T_L^j:

$$T_S^j=T_S^{j-1}+\frac{H_S}{\beta v_S}\left(\Delta T^{j-1}-\frac{\alpha}{\beta}\right)[\exp(-\beta\Delta x)-1] + \left(\frac{G_S}{v_S}-\frac{\alpha}{\beta}\frac{H_S}{v_S}\right)\Delta x \tag{21}$$

and

$$T_L^j=T_S^j-\left[\frac{\alpha}{\beta}+\left(\Delta T^{j-1}-\frac{\alpha}{\beta}\right)\exp(-\beta\Delta x)\right] \tag{22}$$

where

$$\alpha=\frac{G_S}{v_S}-\frac{G_L}{v_L},\quad \beta=\frac{H_L}{v_L}+\frac{H_S}{v_S},\quad \Delta T^j=T_S^j-T_L^j, \tag{23}$$

(iii) Solution of Eqs. 21-23 gives the temperature distribution up the tube, from which the electrical conductivities in each section and the effective conductivity can be found. The mean current density is then given by:

$$C=\frac{\Delta V}{\Delta x\sum_{j=1}^{N}\frac{1}{\kappa_{\mathrm{eff}\,j}}} \tag{24}$$

(iv) This current density can then be used to reestimate the mean field strength in each section to be used in Eq. 6 using:

$$E_j=C/\kappa_{\mathrm{eff}\,j} \tag{25}$$

(v) New temperatures in each section can then be calculated and the current density recalculated using Eq. 24. Iteration continues until successive values of C agree to the required accuracy.

The above procedure applies to a single-section heater; similar principles can be applied to each section of a multiple-section heater, such as the commercial APV Baker ohmic heater.

Holding and Cooling Section

Thermal balances

In the holding and cooling sections of the process, there is no heat generation and it is no longer possible to assume

Table 1. Flow and Physical Property Data for Particle-Liquid Mixtures, 18% Solids

	Velocity (m/s)	Specific Heat (J/kg·K)	Diameter (m)	Fraction of Mixture
Particle 1	0.08	3,857	0.008	0.0324
Particle 2	0.03	3,857	0.008	0.0576
Particle 3	0.01	3,857	0.008	0.09
Liquid	0.06	4,200		0.72

uniform particle temperature. When calculating the temperatures of the two phases, there is, however, no need to solve the field equations, so the problem is more straightforward.

The one-dimensional enthalpy balance approach is again used. The holding or cooling tube is split into sections, each containing a representative number of spherical particles depending on the solids fraction of each. In each section, the liquid temperature is uniform.

For an individual spherical particle of radius R_P, thermal conductivity λ_s and surface temperature T_s^R traveling at velocity v_S in a fluid flowing at a uniform temperature T_L, the intraparticle conduction equation is written as:

$$\frac{1}{r^2}\frac{\partial}{\partial r}\left(\lambda_s r^2 \frac{\partial T_S}{\partial r}\right) = (\rho C_p)_S v_S \frac{\partial T_S}{\partial x} \tag{26}$$

based on radial coordinates from the center of the particle, with the interfacial boundary condition:

$$-h(T_S^0 - T_L) = \lambda_s \left(\frac{dT_S}{dr}\right)_{r=R_p} \tag{27}$$

The enthalpy balance on the liquid side is more complex, since there could be i particles in the section, each with their own physical properties and velocities, exchanging heat with the liquid. For a uniform liquid temperature, T_L, the liquid-phase heat balance becomes:

$$\frac{\sum_i \phi_i h_i a_i (T_{Si}^0 - T_L)}{\left(1 - \sum_i \phi_i\right)} + A_W h_W (T_L - T_W) = v_L (\rho C_p)_L \frac{dT_L}{dx} \tag{28}$$

an equation which takes account of heat transfer to i particles in the section in the first term on the lefthand side. The second term on the lefthand side of Eq. 28 is a wall heat-transfer term, which applies in the cooling stage. T_W is the wall temperature and h_W the wall-fluid heat-transfer coefficient. A_W is the area of heat-transfer surface per unit volume of the heat-transfer equipment; for a pipe of diameter d, $A_W = 4/d$.

Equations 26 and 28 were solved numerically using a finite difference scheme. The pipe was divided into N sections. Within each, the intraparticle conduction (Eq. 26) was solved using a NAG routine, and Eq. 28 rewritten using a central difference method. Inlet temperatures to each section are known; in section j, the liquid temperature is first assumed to be T_L^{j-1}, and the NAG routine is then called to calculate the solid temperatures in each of the particle fractions. Using Eq. 28 together with T_L^{j-1}, and T_S^{j-1} and T_S^j for each particle, the liquid temperature T_L^j can then be calculated.

Once the temperature distributions of the solid and liquid have been calculated along the holding tube and cooling section, the total lethality and product quality can be calculated from the temperature-time profile of each part of the system. Different particle velocities and thus residence times will give rise to particles which have received different thermal treatments.

Flow of food materials

To obtain data relevant to the flows in commercial holding tubes, experiments have been conducted in a horizontal test section of 5 m of perspex pipe of 44 mm ID (Liu et al., 1992, 1993). Preliminary experiments were conducted to examine the flow behavior of single particles of various shapes: spheres, cubes, cylinders, and discs (Liu et al., 1992). Subsequent experiments to study the flow of 8-mm carrot cubes in water at up to 35% delivered solids concentration are described by Liu et al. (1993). The densities of the carrots ranged mainly between 1,010 and 1,080 kg/m^3. Three tracers of the same diameter and specific gravities 1.015, 1.028, and 1.042, were used to represent the behavior of different fractions of the solid.

Here, data from the above study are used to demonstrate the effects which may arise during processing due to differences in particle velocity. Table 1 gives data for a flow of 8-mm cubic carrots of 18% solids fraction in which a large range of velocities is found. Data are given for three fractions of the solids, each of different density. The flow is represented in terms of these three fractions, which each move at a characteristic speed, and comparisons between the behavior of the three fractions of particle made. The variations among velocities are probably higher than they would be industrially; however, they indicate the type of flows that might be seen.

Results and Discussion

Heating section

The model has been used to determine the magnitude of temperature differences which might occur during commercial operation. The first case chosen is one where the solid and liquid have the same variation of electrical conductivity with temperature. It might be thought that in this case both phases will heat equally, but, as shown in Eqs. 2 and 4, it is the inherent heating rate, G, rather than the heat generation, which determines the rate of temperature increase in practice. Two situations, in which the thermal capacity of the particle differs by 10% from the liquid, whose thermal capacity is kept constant, have been simulated in Figure 3.

Details of the physical properties used are given in Table 2; conditions are of relevance to the industrial situation. For simplicity, a single heater tube, rather than the several sections used in the APV system, has been simulated. The particle-liquid heat-transfer coefficient, which is unknown, has been estimated using the conservative limit of $Nu = 2$. Results are shown in Figure 3. In both cases, the two phases heat smoothly, but in Figure 3a, where the solid has a greater thermal capacity, it underheats the liquid, while when it has a greater thermal capacity (Figure 3b) the solid overheats the liquid. Liquid and solid temperatures are effectively reversed between Figures 3a and 3b. In both cases, the difference between the two tem-

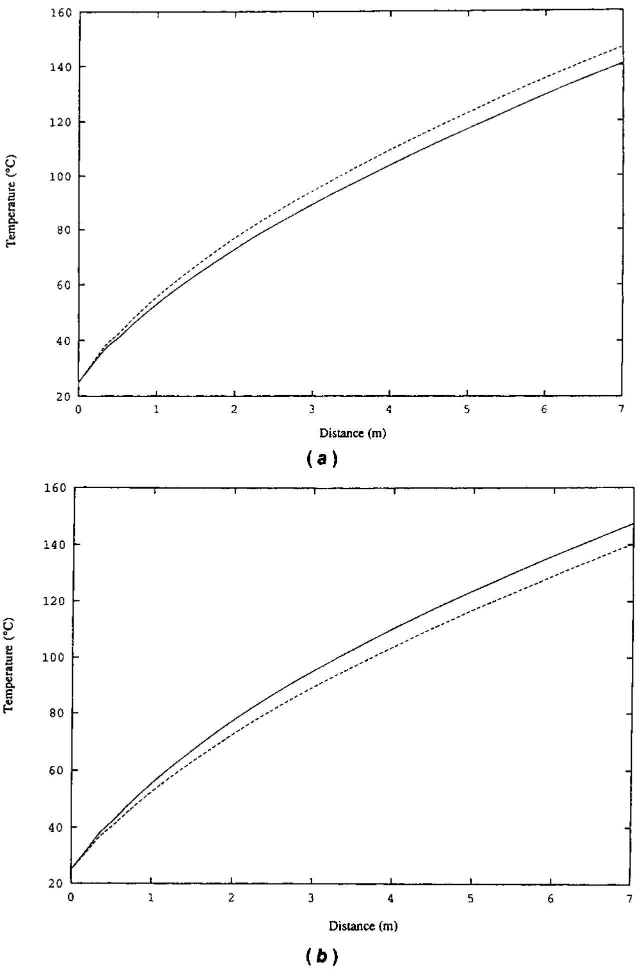

Figure 3. Heating curves for solid and liquid for Table 1 showing the effect of the thermal capacity of the solid.

(a) Solid underheats when its thermal capacity is 10% greater than the liquid; (b) solid overheats when its thermal capacity is 10% less than the liquid. In both cases, solid line shows solid temperature, dotted line shows liquid temperature.

peratures is about 5°C at the end of the heater tube. To have the particle overheating the liquid is the safer operating strategy, as it is easier to measure the liquid temperature, so if it is known that the liquid temperature is the lowest in the system, then the process can be easily controlled.

More commonly, particle and liquid conductivities will be different functions of temperature. Table 3 shows conditions where, at low temperature, the particle is less conductive than the liquid, but at higher temperature becomes more conductive.

Table 2. Data for Simulations of Heating of Spherical Particles in 50% Solids Fraction Flow and Same κ-T Relationship for Both Phases Plotted in Figure 3

Voltage gradient = 1,800 V/m Tube Length = 7m
Particle diameter = 0.02 m $ha = 19{,}500$ W/m^3·K
Thermal capacity of liquid = $(\rho c_p)_L = 4{,}200$ kJ/m^3·K
Thermal capacity of solid = $(\rho c_p)_S = 4{,}620$ kJ/m^3·K (Fig. 3a)
3,780 kJ/m^3·K (Fig. 3b)
Electrical conductivity of both phases
$= \kappa = 0.44[1 + 0.01(T - 22)]$ S/m (T is in °C)
$v_S = v_L = 0.03$ m/s
$T_S^o = T_L^o = 25$°C

Table 3. Data for Simulations of Heating of Spherical Particles in 50% Solids Fraction Flow and Different κ-T Relationship for Two Phases Plotted in Figures 4 and 5

Voltage gradient = 1,950 V/m Tube Length = 7 m
Particle diameter = 0.02 m $ha = 19{,}500$ W/m^3·K
Thermal capacity = $(\rho c_p)_L = (\rho c_p)_S = 4{,}000$ kJ/m^3·K
Electrical conductivity:
$\kappa_S = 0.04[1 + 0.375(T - 22)]$ S/m (T is in °C)
(data for potato from Sastry, 1992)
$\kappa_L = 0.62[1 + 0.01(T - 22)]$ S/m (T is in °C)
$v_S = v_L = 0.03$ m/s
$T_S^o = T_L^o = 25$°C

For the solid, data for potato have been used; the liquid conductivity can take any level by the addition of appropriate salts. Figure 4 shows the more complex heating pattern that results: at low temperatures the solid lags behind the liquid, while at higher temperature it catches up and then overtakes the liquid temperature as its conductivity rises. More marked effects would be seen if the k-T relationship were nonlinear; Halden et al. (1990) suggest that cellular breakdown may result in significant increases in conductivity over narrow temperature ranges in electrical heating.

The heating model has been developed assuming uniform temperatures in the two phases. It is instructive to plot the ratio of the amount of heat transfer to a particle as a ratio of the heat generation within the particle defined as:

$$Z_\Omega = \frac{\pi d^2 h(T_S - T_L)}{\frac{\pi d^3}{6} Q_S} = \frac{6h(T_S - T_L)}{dQ_S} \qquad (29)$$

Figure 5 shows this ratio for the data of Table 3. Z_Ω changes sign at the point in the column where the solid becomes hotter than the liquid. The heat generation term always dominates, demonstrating that the assumptions of the model are sound.

Simulations suggest that it will be difficult in practice to equalize solid and liquid output temperatures during electrical heating. The result is not sensitive to the particle-liquid heat-transfer coefficient, because of the high Biot number of the

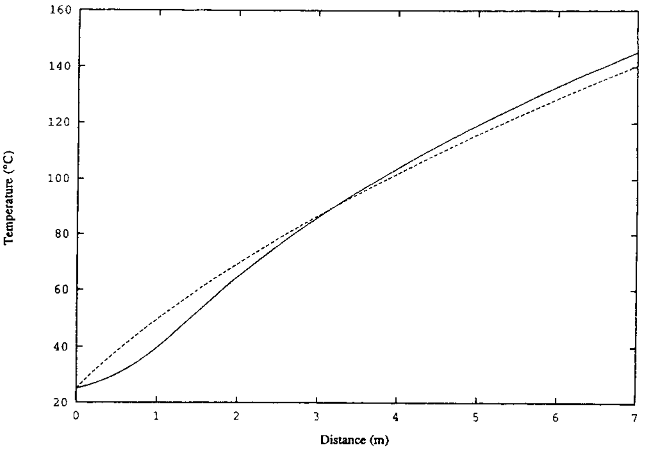

Figure 4. Heating curves for solid and liquid for Table 2 showing the effect of electrical conductivity crossover on the heating of the two phases.

Solid line shows solid temperature, dotted line shows liquid temperature.

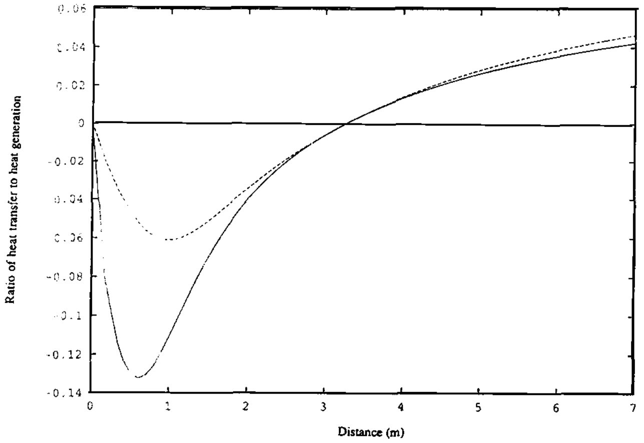

Figure 5. Ohmic ratio defined in Eq. 28 for Figure 4, showing the relative effect of heat transfer and heat generation in electrical heating.

Solid line shows Eq. 28 for the solid, dotted line for the liquid.

solid and the small Z_Ω. The effect of varying other process parameters is more important. Food physical properties are inherently variable; it is felt that the thermal capacity and electrical conductivity of the solid could well vary by up to 10% in practice. Simulations were carried out to study the effect of changing the thermal capacity of the two phases, for the base conditions of Table 1, on the outlet temperatures from the heating column. This resulted in temperature changes of 10°C in the solid and 4°C in the liquid; if the capacity increased, the temperature of the corresponding phase decreased, and vice versa. A 10% change in the electrical conductivity of the solid changed temperatures by about 5°C. It is felt that such temperature changes could be seen in practice. The next section shows what effect this might have.

Holding section

Variations in the outlet temperature from the heating tube might be of the order of ±5-10°C in a commercial situation. Equations 28-30 have been solved to study temperature changes in the holding tube. The experimental velocity data of Table 1 have been used to represent possible ranges in particle residence time. Adiabatic operation has been assumed: $h_w = 0$ in Eq. 30; the physical property data for Table 1 have also been used.

Since the only mechanism for heat transfer in the holding section is thermal conduction ($Z_\Omega = \infty$), it is not possible to assume that the particle temperature is uniform. Figure 6 shows the thermal response of particle 1, traveling at 0.08 m/s, for the case where its inlet temperature is a uniform 120°C and the liquid temperature is 140°C. As would be expected, although the surface temperature ($r = 0.004$ m) changes quickly, the particle center temperature does not change rapidly. Holding tubes for conduction processing of solid-liquid mixtures effectively serve two purposes; they allow the temperature of the solid to reach a temperature at which the sterilization reaction takes place rapidly and then allow enough time at high temperature for the sterilization reaction to proceed to the required extent. If the temperatures of both phases are matched by electrical heating, then much shorter holding tubes will be needed.

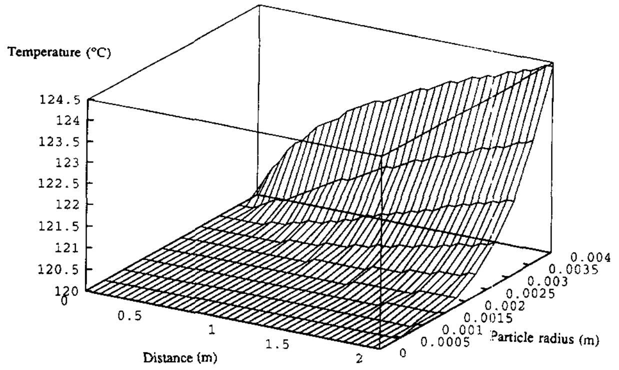

Figure 6. Thermal response of a particle of diameter 8 mm and velocity of 0.08 m/s, starting temperature 120°C, to a fluid at 140°C.

Simulations have studied the range of effects which might be seen in commercial plant for the three particle fractions in Table 1. The required F value for the product was chosen as $F_p = 10$ min and calculated using Eq. 12, $T_{ref} = 121.6$°C, and $z = 10$°C. Figure 7 is plotted in terms of $\phi_F = F/F_p$: for $\phi_F > 1$, the food is of the required sterility and is expressed as the change in ϕ_F at the center of the particle as a function of

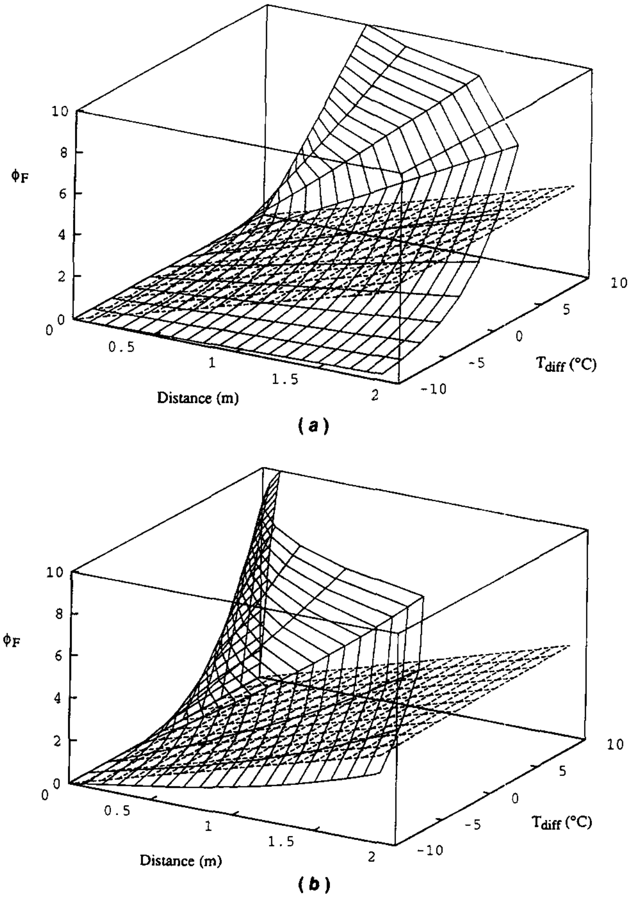

Figure 7. Sterility ratio ϕ_F plotted as a function of distance along the hold tube and T_{diff} for constant liquid inlet temperature of 140°C and Table 1: (a) particle 1; (b) particle 3.

In each case, solid lines show particle sterilization, dotted lines show liquid.

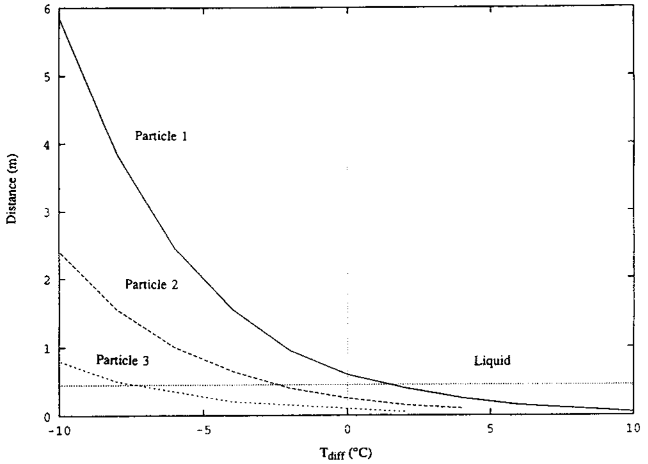

Figure 8. Length of hold tube required to sterilize the materials of Table 1 as a function of T_{diff} for constant liquid inlet temperature of 140°C.

distance down the hold tube and the initial temperature difference between the two phases, defined as:

$$T_{diff} = T_S^0 - T_L^0 \tag{30}$$

Figures 7a and 7b show the effect of T_{diff} varying between ±10°C, for a constant liquid inlet temperature of 140°C, for particles 1 and 3 of Table 1. Clear differences in the shape of the curves can be seen between Figure 7a, where the particle travels faster than the liquid, and Figure 7b where the particle travels slower than the liquid. The F value is very sensitive to temperature. The speed of particle 1 in Figure 7a is such that it is significantly underprocessed with respect to the liquid for all cases when it underheats the liquid, while for particle 3, which travels slower than the liquid, Figure 7b shows that it can have a higher F value than the liquid in the same part of the tube, even when T_{diff} is negative.

Figure 8 shows the data of Figure 7 in more directly useful form. Here, the length of hold tube is required to sterilize the three particles and the liquid as a function of the temperature difference between the phases. In general, when the particle is colder than the liquid, the last point to be sterilized is the center of the particle; however, for positive T_{diff}, the liquid is the last phase to be sterilized. This diagram displays the fraction of the fluid which is most difficult to sterilize in any given case. When the temperatures of the phases are the same, the length of the hold tube is set by particle 1, which travels faster than the liquid; however, if the particle exceeds the liquid temperature by more than a degree, then the liquid is the last phase to be sterilized, and the length of the hold tube is set by the need to process the liquid. For particles which underheat the liquid, however, a much greater holding tube length is necessary; for those cases, as shown in Figure 7, significant overprocessing of the liquid will result. Here, the effect of the velocity of the particle is much more obvious; if the rapidly moving particle 1 is underheated, then a significantly longer hold tube is needed than if the slower particle 3 is underheated.

It should be noted that Table 1 is for 18% solids and gives a wider range of velocities than would be found with higher solids fractions. If the velocities in the system were closer to plug flow, then the effects of temperature will become even more dominant; for example, the recovery of F possible for the slowest particles would not occur. The simulations show clearly that only slight overheating is needed to allow the liquid phase to be the last to be sterilized; however, it is uncertain whether such tight temperature control can be found in practice.

Discussion

The model for the electrical heater developed here has allowed process temperatures to be estimated for variations in physical properties similar to those found in practice. The variation in electrical conductivity with temperature has a very significant effect on phase heating rates. The results presented here demonstrate the range of thermal effects which are likely to occur in a commercial electrical processing plant. The model for heating is an approximate one; it is important to get data for a real system to see whether the approximations are appropriate in practice. However, it is felt that the heating effects predicted by the model are correct in outline as they are similar to those seen in previous experimental work (de Alwis et al., 1989; Halden et al., 1990). It is important that any commercial unit should be able to cope with natural variations in electrical conductivity found in foods and thus with temperature differences similar to those found here. The model for the holding tube shows that at these high temperatures very small hold tubes are needed to give the required process level. It may be that at 140°C the need to design to account for, say, ±5°C in particle temperature gives an unacceptable variation in the range of product qualities and that a lower process temperature is better. However, when hold tube length for a base case of 135°C, instead of 140°C, is calculated, an essentially identical set of curves as Figure 7 is found, except that a longer hold tube is required; as before, when the particles underheat the liquid, a very much longer hold tube is required. The design of hold tubes remains a difficult problem for which more data are needed on the temperatures and velocities which are found in practice. One possible solution might be to ensure that the particle velocity is sufficiently less than the liquid that the two phases, despite different entrance temperatures, are both sterile at the exit.

One major problem in any model is that the heat-transfer coefficients between particle and liquid are not well characterized. The 'ohmic ratio' defined in Eq. 32 is potentially useful for determining the relative effect of heat transfer and generation in the system. Mwangi et al. (1992, 1993) discuss heat transfer in flowing systems and quote a number of experimental results for single particles and solids fractions up to 5%. Chang and Toledo (1990) describe measurements of heat transfer within a packed bed of diced carrot to simulate the high solids fractions found in practice and found evidence that the limiting heat-transfer coefficient in a packed bed is higher than the $Nu = 2$ predicted from single-particle heat-transfer data, similar to that noted for packed beds in the process industries; similar indications were found by Mwangi et al. (1993). The controlling factor would be expected to be the particle-liquid slip velocity; for low slip, the conduction limit will be approached, while at higher velocities higher heat-transfer coefficients will be found. For high heat-transfer coefficients, thermal conduction will control the particle response, but it may well be that in the slow flows found in commercial plants the particle-liquid heat-transfer coefficient influences the process time. Here, $Nu = 2$ has been used throughout; further work is underway to determine whether correlations appropriate for a single particle are accurate in these systems.

Significantly more computing power would be needed to produce a model that takes account of thermal conduction as well as heat generation. Rather than using correlations for the heating rate, an improved model should incorporate a finite element simulation of a unit cell into the iterative scheme; such a model would also deal with the shape and orientation effects which result when differently shaped food particles are used. The model has considered only spherical particles, while a real food material will contain a variety of shapes; a new set of correlations would be needed for each different shape of particle. Particles with large aspect ratios will have a heating rate that depends significantly on their orientation to the field (de Alwis et al., 1989; Sastry and Palaniappan, 1992); in this case, it may be necessary to investigate a unit cell which contains particles in the two limiting orientations, parallel to and at right angles to the current flux.

Conclusions

Continuous food sterilization plants consist of heating, holding and cooling sections. It is vital to predict temperature distributions in such systems, since the rate at which a product becomes sterile depends on temperature.

A model for the electrical heating of solid-liquid food mixtures has been constructed which can cope with the natural variations in physical properties found in real food systems. The heat generation rate in the two phases has been found by solving Laplace's equation in a 'unit cell' of the fluid; correlations have been derived for the heating rate as a function of the solid and liquid electrical conductivity. This model has been applied to the common practical case of significant variation in the ratio of electrical conductivities along the column, and demonstrates that it is very difficult to produce a mixture of uniform temperature at the exit of the heating section.

Experimental work has been carried out to characterize flows of solid-liquid mixtures in horizontal tubes. It has been shown that it is possible to obtain significant velocity differences between particles. The subsequent effect of variation in heating temperature in holding tubes has been studied using an enthalpy balance model to calculate solid and liquid temperatures and the resulting rates of sterility for a mixture containing three types of particle, each moving at a different velocity. Depending on the temperatures, sterilization of either solid or liquid phase can be the slowest and control the length of the hold tube. The ideal operation of the system seems to be that particle temperature should exceed the liquid by a slight amount, less than a degree. It is uncertain whether this could be achieved in practice. Further work is necessary both to verify the model in an experimental situation and to determine the effect which particle-liquid heat-transfer coefficients have on the overall process.

Acknowledgment

LZ wishes to acknowledge financial support from AFRC. ANSYS was supplied at an academic rate by Strucom Ltd., Croydon, UK. Original work on electrical heating at Cambridge was supported by APV Baker Ltd, and work on particle flow was supported by Sous-Chef Ltd.

Notation

a = area per unit volume of particle (m^{-1})
a_1, a_2, a_3, a_4, a_5 = constants
A = area
c_p = specific heat ($kJ \cdot kg^{-1} \cdot K^{-1}$)
d = particle diameter (m)
D = pipe diameter (m)
E = mean electric field strength ($V \cdot m^{-1}$)
E = electric field intensity ($V \cdot m^{-1}$)
$f_{1,2}$ = functions
F = sterilization factor defined by Eq. 10 (s or min)
F_p = target process F value (s or min)
G = inherent heating rate ($°C \cdot s^{-1}$)
h = heat-transfer coefficient ($W \cdot m^{-2} \cdot K^{-1}$)
H = modified heat-transfer term (s^{-1})
i = number of particle
j = number of tube section
k_0, k_1 = constants defined by Eq. 18
L = length of tube (m)
N = total number of tube sections
Q = heat generation rate ($W \cdot m^{-3}$)
Q_1 = heat generation rate for single-phase liquid ($W \cdot m^{-3}$)
r = radial coordinate (m)
R = ratio
R_p = particle radius (m)
R_Q = heat generation ratio
R_κ = conductivity ratio
t = time (s)
t_{proc} = process time (s)
T = temperature (K)
v = velocity ($m \cdot s^{-1}$)
V = voltage (V)
x = distance (m)
z = temperature factor for sterilization in Eq. 12 (°C)
Z_Ω = ohmic ratio defined in Eq. 28

Greek letters

α = factor defined in Eq. 23 ($°C \cdot s^{-1}$)
β = factor defined in Eq. 23 ($°C \cdot s^{-1}$)
δ_F = factor in Eq. 10 = $\ln(10)/z$ ($°C^{-1}$)
ΔL = length of tube segment (m)
ΔT = difference between solid and liquid temperature (°C)
ΔV = voltage drop ($V \cdot m^{-1}$)
ΔV_{tot} = voltage drop ($V \cdot m^{-1}$)
Δx = edge size of unit cell (m^{-1})
κ = electrical conductivity ($S \cdot m^{-1}$)
ϕ = solids fraction
ϕ_F = sterilization ratio, defined by Eq. 2
ϕ_i = fraction of component i
λ_s = thermal conductivity ($W \cdot m^{-1} \cdot K^{-1}$)
ρ = density ($kg \cdot m^{-3}$)

Subscripts and superscripts

diff = difference
e = exit
eff = effective
i = particle i
j = section j
L = liquid
n = section n
o = inlet or initial
OUT = outlet
R = radius R
ref = reference
S = solid
W = wall
κ = conductivity

Literature Cited

Ayappa, K. G., H. T. Davis, G. Crapiste, E. A. Davis, and J. Gordon, "Microwave Heating—an Evaluation of Power Formulations," *Chem. Eng. Sci.*, **46**, 1005 (1991).

Biss, C. H., S. A. Coombes, and P. J. Skudder, "The Development and Application of Ohmic Heating for the Continuous Heating of Particulate Foodstuffs," *Engineering Innovation for the Food Industry*, J. A. Howell and R. A. Field, eds., Elsevier, London (1990).

Chang, S. Y., and R. T. Toledo, "Simultaneous Determination of Thermal Diffusivity and Heat Transfer Coefficient during Sterilisation of Carrot Dices in a Packed Bed," *J. Food Sci.*, **55**, 199 (1990).

de Alwis, A. A. P., and P. J. Fryer, "Operability of the Ohmic Heating Process: Electrical Conductivity Effects," *J. Food Eng.*, **15**, 21 (1992).

de Alwis, A. A. P., K. Halden, and P. J. Fryer, "Shape and Conductivity Effects in the Ohmic Heating of Foods," *Chem. Eng. Res. Des.*, **67**, 159 (1989).

de Alwis, A. A. P., L. Zhang, and P. J. Fryer, "Modelling Sterilisation and Quality of the Ohmic Heating Process," *Advances in Aseptic Processing Technologies*, R. K. Singh and P. E. Nelson, eds., Elsevier, London (1992).

Dutta, B., and S. K. Sastry, "Velocity Distributions of Food Particle Suspensions in Holding Tube Flow: Distribution Characteristics and Fastest-Particle Velocities," *J. Food Sci.*, **55**, 1703 (1990a).

Dutta, B., and S. K. Sastry, "Velocity Distributions of Food Particle Suspensions in Holding Tube Flow: Experimental and Modelling Studies on Average Particle Velocities," *J. Food Sci.*, **55**, 1448 (1990b).

Fryer, P. J., A. A. P. de Alwis, E. Koury, A. G. F. Stapley, and L. Zhang, "Ohmic Heating of Solid-Liquid Foods: Heat Generation and Convection Effects," *J. Food Eng.*, **18**, 101 (1993).

Halden, K., A. A. P. de Alwis, and P. J. Fryer, "Changes in Electrical Conductivity of Foods During Ohmic Heating," *Int. J. Food Sci. Technol.*, **25**, 9 (1990).

Holdsworth, S. D., *Aspetic Processing and Packaging of Food Products*, Elsevier, London (1993).

Heppel, N. J., "Comparison of the Residence Time Distributions of Water and Milk in an Experimental UHT Steriliser," *J. Food Eng.*, **4**, 71 (1985).

Liu, S., J.-P. Pain, and P. J. Fryer, "The Flow and Velocity Distributions of Single Particles in Liquids and Their Application in Food Processing," *Entropie*, **28**, 50 (1992).

Liu, S., J.-P. Pain, J. M. Proctor, A. A. P. de Alwis, and P. J. Fryer, "An Experimental Study of Particle Flow Velocities in Solid-Liquid Food Mixtures," *Chem. Eng. Commun.*, in press (1993).

McKie, D. M., and C. H. McKie, *Fundamentals of Crystallography*, Wiley, New York (1986).

Mwangi, J. M., A. K. Datta, and S. S. H. Rizvi, "Heat Transfer in Aseptic Processing of Particulate Foods," *Advances in Aseptic Processing Technologies*, R. K. Singh and P. E. Nelson, eds., Elsevier, London (1992).

Mwangi, J. M., A. K. Datta, and S. S. H. Rizvi, "Heat Transfer to Particles in Shear Flow; Application in Aseptic Processing," *J. Food Eng.*, **19**, 55 (1993).

Parrott, D. L., "Use of Ohmic Heating for Aseptic Processing of Particulates," *Food Technol.*, 68 (Dec., 1992).

Rao, M. A., and M. Loncin, "Residence Time Distribution and Its Role in Continuous Pasteurisation," *Lebesnm. Wiss. u-Techn.*, **7**, 4 (1974).

Sancho, M. F., and M. A. Rao, "Residence Time Distribution in a Holding Tube," *J. Food Eng.*, **15**, 1 (1992).

Sastry, S., "A Model for Heating of Liquid-Particle Mixtures in a Continuous Flow Ohmic Heater," *J. Food Proc. Eng.*, **15**, 263 (1992).

Sastry, S., and S. Palaniappan, "Influence of Particle Orientation on the Effective Electrical Resistance and Ohmic Heating Rate of a Liquid-Particle Mixture," *J. Food Proc. Eng.*, **15**, 213 (1992).

Sawinski, J., and B. Simandi, "The Residence Time Distribution for Laminar Flow of a Non-Newtonian Fluid in a Straight Circular Flow," *Trans. IChemE*, **60**, 67 (1982).

Singh, R. K., and J. H. Lee, "Residence Time Distributions of Foods with/without Particulates in Aseptic Processing Systems," *Advances in Aseptic Processing Technologies*, R. K. Singh and P. E. Nelson, eds., Elsevier, London (1992).

Wilson, K. C., "Pipeline Design for Settling Slurries," *Slurry Handling Design for Solid-Liquid Systems*, N. P. Brown and N. I. Heywood, eds., Elsevier, London (1991).

Zhang, L., and P. J. Fryer, "Models for the Electrical Heating of Solid-Liquid Food Mixtures," *Chem. Eng. Sci.*, **48**, 633 (1993).

Zhang, L., and P. J. Fryer, "Alternative Formulations for the Prediction of Electrical Heating Rates of Solid-Liquid Food Materials," *J. Food Proc. Eng.*, in press (1994).

Manuscript received Apr. 28, 1993, and revision received July 26, 1993.